HFE H63D Limits Nigral Vulnerability to Paraquat in Agricultural Workers

Ernest W. Wang,* Max L. Trojano,* Mechelle M. Lewis,*,† Guangwei Du,*
Hairong Chen,* Gregory L. Brown,* Leslie C. Jellen,* Insung Song,‡
Elizabeth Neely,‡ Lan Kong,§ James R. Connor,‡ and Xuemei Huang*,†,‡,¶,‖,1

*Department of Neurology, Pennsylvania State Health-Milton S. Hershey Medical Center, Hershey, Pennsylvania 17033, USA; †Department of Pharmacology, Pennsylvania State Health-Milton S. Hershey Medical Center, Hershey, Pennsylvania 17033, USA; ‡Department of Neurosurgery, Pennsylvania State Health-Milton S. Hershey Medical Center, Hershey, Pennsylvania 17033, USA; §Department of Public Health Sciences, Pennsylvania State Health-Milton S. Hershey Medical Center, Hershey, Pennsylvania 17033, USA; ¶Department of Radiology, Pennsylvania State Health-Milton S. Hershey Medical Center, Hershey, Pennsylvania 17033, USA and ‖Department of Kinesiology, Pennsylvania State Health-Milton S. Hershey Medical Center, Hershey, Pennsylvania 17033, USA

Ernest W. Wang and Max L. Trojano contributed equally to this study.

The authors certify that all research involving human subjects was done under full compliance with all government policies and the Helsinki Declaration.

[1]To whom correspondence should be addressed at Department of Neurology, Pennsylvania State Health-Milton S. Hershey Medical Center, H037, 500 University Dr, Hershey, PA 17033-0850, USA. E-mail: xuemei@psu.edu.

ABSTRACT

Paraquat is an herbicide whose use is associated with Parkinson's disease (PD), a neurodegenerative disorder marked by neuron loss in the substantia nigra pars compacta (SNc). We recently observed that the murine homolog to the human H63D variant of the homeostatic iron regulator (*HFE*) may decrease paraquat-associated nigral neurotoxicity in mice. The present study examined the potential influence of H63D on paraquat-associated neurotoxicity in humans. Twenty-eight paraquat-exposed workers were identified from exposure histories and compared with 41 unexposed controls. *HFE* genotypes, and serum iron and transferrin were measured from blood samples. MRI was used to assess the SNc transverse relaxation rate (R2*), a marker for iron, and diffusion tensor imaging scalars of fractional anisotropy (FA) and mean diffusivity, markers of microstructural integrity. Twenty-seven subjects (9 exposed and 18 controls) were H63D heterozygous. After adjusting for age and use of other PD-associated pesticides and solvents, serum iron and transferrin were higher in exposed H63D carriers than in unexposed carriers and *HFE* wildtypes. SNc R2* was lower in exposed H63D carriers than in unexposed carriers, whereas SNc FA was lower in exposed *HFE* wildtypes than in either unexposed *HFE* wildtypes or exposed H63D carriers. Serum iron and SNc FA measures correlated positively among exposed, but not unexposed, subjects. These data suggest that H63D heterozygosity is associated with lower neurotoxicity presumptively linked to paraquat. Future studies with larger cohorts are warranted to replicate these findings and examine potential underlying mechanisms, especially given the high prevalence of the H63D allele in humans.

Key words: paraquat; *HFE*; H63D; iron; MRI; DTI.

Paraquat (1,1′-dimethyl-4,4′-bipyridium) is an herbicide used widely in agricultural settings across the United States (Baker, 2016). Its usage is controversial, however, as exposure is associated with an increased risk for Parkinson's disease (PD) (Pezzoli and Cereda, 2013; Tanner *et al.*, 2011; Wang *et al.*, 2011). PD is a neurodegenerative movement disorder characterized by loss of dopaminergic neurons in the substantia nigra (SN), specifically the pars compacta (SNc). Paraquat has been shown to target the SNc via uptake through regionally expressed dopamine transporters (Rappold *et al.*, 2011). Exposure of mice and rats to paraquat results in SN neuronal loss and motor function deficits reminiscent of PD (Brooks *et al.*, 1999; Manning-Bog *et al.*, 2002; Ossowska *et al.*, 2005). Although there have been mixed findings regarding these effects and paraquat's associations to PD, the overall weight of literature suggests a role for paraquat in PD, as previously reviewed and discussed (Cook *et al.*, 2014; Jones *et al.*, 2014a,b).

Recent research has demonstrated that diffusion tensor imaging (DTI), an MRI-based neuroimaging technique, is sensitive to PD-related microstructural changes in the SN (Atkinson-Clement *et al.*, 2017). Using DTI, we have demonstrated that asymptomatic agricultural workers exposed to paraquat had lower SN fractional anisotropy (FA) than their unexposed counterparts (Du *et al.*, 2014). This microstructural change was similar (lower magnitude) to that observed in PD patients (Atkinson-Clement *et al.*, 2017; Du *et al.*, 2014). Because an estimated 30% of dopamine neurons are lost before motor symptoms emerge in PD (Cheng *et al.*, 2010), this data suggests that SN FA changes in paraquat-exposed workers may reflect preclinical degeneration.

Intracellularly, paraquat exerts toxicity through reduction-oxidation (redox) cycling (Figure 1A) to increase cellular oxidative stress (Suntres, 2002). In a physiological medium, paraquat (PQ^{2+}) can accept an electron from a reducing equivalent (eg, NADH, NADPH) through cytosolic and mitochondrial reductive enzymes (Cocheme and Murphy, 2008; Gray *et al.*, 2007; Shimada *et al.*, 1998). The resulting free radical ($PQ^{\bullet+}$) is oxidized back to its PQ^{2+} state in the presence of oxygen (O_2), converting O_2 into the reactive oxygen species (ROS) superoxide ($O_2^{\bullet-}$). $O_2^{\bullet-}$ may be converted sequentially into hydrogen peroxide (H_2O_2) and the hydroxyl radical ($^{\bullet}OH$) through superoxide dismutase (SOD) and Fenton-like reactions, respectively (Figure 1B) (Reczek *et al.*, 2017). Thus, paraquat increases oxidative stress and also depletes neurons of reducing equivalents. These processes together may lead to neuron death (Suntres, 2002).

Another disease-influencing factor in the SN is iron, which is present at higher concentrations in the SN than in other brain regions. Like paraquat, iron is a redox agent. In excess, iron may generate ROS, as in the Fenton reaction (Figure 1C), to mediate harmful oxidation of lipids, proteins, and DNA, and influence neuron death (Carocci *et al.*, 2018; Snyder and Connor, 2009; Ward *et al.*, 2014). Iron and paraquat treatments have been shown to potentiate each other to enhance murine SNc neuron loss and microglial activation (Peng *et al.*, 2007, 2009). It previously was shown that SN neuron loss after paraquat exposure varies among inbred strains of mice despite equal paraquat distribution in the midbrain (Yin *et al.*, 2011). This was associated with differential expression of genes involved in iron metabolism, suggesting that iron, and factors that regulate it, may play a role in paraquat neurotoxicity.

The human homeostatic iron regulator (*HFE*) is one possible gene modifier because common *HFE* mutations explain
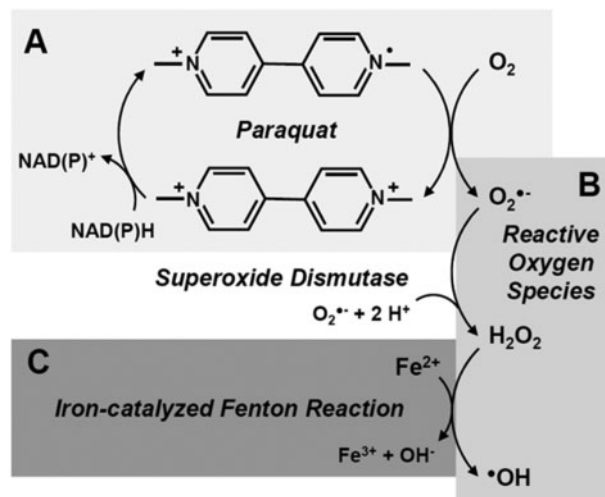

Figure 1. Paraquat redox cycling and generation of reactive oxygen species (ROS). (A) Paraquat cycles between oxidation states by accepting an election from reducing equivalents such as NAD(P)H, and donating an electron to oxygen (O_2). (B) Electron donation to O_2 results in the formation of superoxide ($O_2^{\bullet-}$), the precursor of other ROS. Superoxide dismutase catalyzes the conversion of $O_2^{\bullet-}$ to hydrogen peroxide (H_2O_2), whereas (C) iron-catalyzed Fenton-like reactions convert H_2O_2 to the hydroxyl radical ($^{\bullet}OH$) (Gray *et al.*, 2007; Reczek *et al.*, 2017) .

significant population variance in iron metabolism (Benyamin *et al.*, 2009). The histidine-to-aspartic-acid substitution at position 63 (H63D) is the most prevalent of these variants and about one-quarter of the U.S. population is either heterozygous or homozygous for this allele (Steinberg *et al.*, 2001). *HFE* encodes a cell-surface, iron-sensing protein that regulates the primary mammalian iron transport mechanisms (Hentze *et al.*, 2010). The H63D variant encodes an *HFE* protein product with partial loss of function (Feder *et al.*, 1997; Waheed *et al.*, 1997). Among H63D carriers, this presents as a mildly elevated blood iron phenotype (Gochee *et al.*, 2002; Jackson *et al.*, 2001).

We recently reported that the murine homolog to H63D decreased paraquat-associated neurotoxicity in mice (Nixon *et al.*, 2018). The present study used existing blood samples and data from earlier experiments (Du *et al.*, 2014; Lewis *et al.*, 2017) to provide initial testing of the hypothesis that *HFE* H63D may limit paraquat-associated neurotoxicity in humans.

MATERIALS AND METHODS

Study subjects. This study included 69 unique subjects who participated in two previous studies related to paraquat-containing pesticide exposure (Du *et al.*, 2014; Lewis *et al.*, 2017). The subjects included 28 paraquat-exposed workers (eg, farmers, landscapers, pesticide-applicators) and 41 unexposed controls. Subjects were recruited from regional agricultural workers meetings in central Pennsylvania, and from the local community surrounding the Pennsylvania State University-Milton S. Hershey Medical Center. Inclusion and exclusion criteria common to the earlier studies were: ability and willingness to provide consent; no significant memory impairment (Mini Mental Status Exam [MMSE] >24); normal kidney and liver function; no present history of acute or chronic medical conditions, or neurological deficits; and no condition precluding an MRI (ie, claustrophobia). The first study (Du *et al.*, 2014) limited enrollment to individuals between the ages of 21 and 75 years, whereas the age limits for the second study (Lewis *et al.*, 2017) were between

45 and 75 years. All subjects who volunteered were male and provided written informed consent for study procedures, including the collection and storage of blood samples for genotyping. Collection of all clinical, laboratory, and imaging measurements was approved by the institutional review board at the Pennsylvania State University-Milton S. Hershey Medical Center, and was conducted in accordance with the Declaration of Helsinki.

Clinical assessments. Subjects completed questionnaires assessing the number of years and days per year they applied paraquat (Du *et al.*, 2014; Lewis *et al.*, 2017). A paraquat exposure metric was generated by multiplying the number of years by days per year of exposure. All subjects also were questioned on their usage of other chemicals with reported association to PD incidence, mortality and/or disease processes, including the pesticides glyphosate (Caballero *et al.*, 2018; Pu *et al.*, 2020), atrazine (Coban and Filipov, 2007; Filipov *et al.*, 2007), maneb (Cicchetti *et al.*, 2005; Costello *et al.*, 2009), rotenone (Betarbet *et al.*, 2000; Tanner *et al.*, 2011), and ziram (Fitzmaurice *et al.*, 2014; Rhodes *et al.*, 2013; Wang *et al.*, 2011), as well as the solvents trichloroethylene (Gash *et al.*, 2008; Goldman *et al.*, 2012) and tetrachloroethylene (Goldman *et al.*, 2012). Subjects were assigned a value of 0 or 1 for usage of any of these chemicals under an "other pesticide/solvent use" variable that was used in later group comparisons. Chemicals were not tested as independent variables in order to minimize the likelihood of overfitting.

In addition to the MMSE, each subject was administered the Montreal Cognitive Assessment (MoCA) to evaluate global cognitive status. Each subject also completed the University of Pennsylvania Smell Identification Test (UPSIT) to assess olfactory function, and the Unified Parkinson's Disease Rating Scale (UPDRS) Parts I, II, and III. UPDRS-I assesses nonmotor symptoms of behavior and mood, whereas UPDRS-II and -III evaluate motor symptoms experienced by subjects in activities of daily living and motor signs observed by a trained specialist, respectively.

Laboratory assessments. Fasting blood samples were drawn at approximately 0800 h from each subject during their study visit. The samples were analyzed by a laboratory iron panel that included serum iron levels, total iron binding content (TIBC), and transferrin saturation. These measures were part of a standard medical assessment used to screen for possible confounding factors in the original previous studies (Du *et al.*, 2014; Lewis *et al.*, 2017). Serum ferritin and transferrin levels were not assessed in these studies.

HFE variant genotyping. All subjects were genotyped for *HFE* H63D. In addition, all were genotyped for the *HFE* cysteine-to-tyrosine substitution at position 282 (C282Y), a variant with known effects on serum iron levels. C282Y is the second most common *HFE* variant in the United States after H63D, but is carried by less than 10 percent of the population (Steinberg *et al.*, 2001). Due to the distinct phenotype of C282Y, it was predetermined that subjects carrying C282Y would be excluded from group comparisons in order to control for this possible confounding factor. DNA samples were extracted from blood samples and genotyped for the H63D and C282Y variants by polymerase chain reaction-restriction fragment length polymorphism analysis as described in Jeng *et al.* (2003).

MRI image acquisition and postprocessing. All study subjects were scanned using a 3 T MRI system (Magnetom Trio; Siemens,

Erlangen, Germany) with high-resolution T1-weighted (T1w), T2-weighted (T2w), susceptibility mapping (T2*-weighted for R2*), and DTI sequences. T1w images were acquired using a 3D MP-RAGE sequence with the following parameters: TR/TE = 1540/2.3 ms, FoV = 256 × 256 mm, matrix = 256 × 256, section thickness = 1 mm (no gap), section number = 176. T2w images were acquired using a fast spin-echo sequence with TR/TE = 2500/316 ms and the same FoV, matrix, section thickness, and section number as the T1w images. T2*-weighted images were acquired using study-dependent multigradient-echo sequences. Parameters for subjects enrolled in the first study (Du *et al.*, 2014) were: 5 echoes with TEs ranging from 8 to 40 ms at an interval of 8 ms, TR = 51 ms, flip angle = 15°, FoV = 230 × 230 mm, matrix = 256 × 256, section thickness = 1.6 mm, section number = 88. Parameters for subjects enrolled in the second study (Lewis *et al.*, 2017) were: 8 echoes with TEs ranging from 6.2 to 49.6 ms at an interval of 6.2 ms, TR = 55 ms, flip angle = 15°, FoV = 240 × 240 mm, matrix = 256 × 256, section thickness = 2 mm, section number = 64. DTI parameters were as follows: TR/TE = 8300/82 ms, b value = 1000 s/mm^2, diffusion gradient directions = 42, 7 b = 0 scans, FoV = 256 × 256 mm, matrix = 128 × 128, section thickness = 2 mm (no gap), section number = 65.

R2* (1/T2*) images were estimated from nonlinear curve fitting of $S(TE) = S_0 e^{-R2^* \cdot TE}$ using the Levenberg-Marquardt approach. DTI images were processed using DTIPrep (NIRAL, UNC-Chapel Hill, North Carolina), where intersection and intervolume correlation analysis, eddy currents, and motion artifact correction were performed for quality control before estimation of FA and mean diffusivity (MD) values. MRIs were examined by an experience neuroimager (G.D.) for structural abnormalities and imaging artifacts that precluded inclusion in the study. Four DTI scans and nine R2* images failed quality control, and therefore were excluded from analyses.

Substantia nigra par compacta segmentation and mapping. Whereas our previous studies used MRI to examine the entire SN, here we focused on the SNc because it is a postulated locus of high paraquat neurotoxicity (Rappold *et al.*, 2011). Left and right SNc were defined on axial sections of a standard MNI152 T2w template (ICBM 2009a, Montreal Neurological Institute, Montreal, Canada) as the bilateral hypointense bands between the red nuclei and cerebral peduncles. Template SNc ROIs were six axial sections thick, with the superior extent one axial section inferior to the section depicting the largest red nucleus radius (Figure 2A) (Du *et al.*, 2014).

Mapping of template SNc ROIs to subjects' R2* images was as follows: (1) subjects' T1w images were affine and nonlinearly registered to the MNI152 T1w template (ICBM 2009a) using FSL FNIRT (FMRIB Software Library, Oxford, UK); (2) the inverse of the above transformation was applied to the template SNc ROIs to map them into subjects' T1w space; (3) subjects' T2*-weighted magnitude images were affine registered to their T1w images; and (4) the inverse of this last transformation was used to map the ROIs in subjects' T1w space to their R2* images (Figure 2B). For DTI, FA maps from each subject were affine and nonlinearly registered to the FMRIB FA58 template (an average of 58 FA maps from healthy subjects in standard MNI152 space). Template SNc ROIs then were mapped to each subjects' scalar images (FA, MD) by applying the inverse transformation (Figure 2C). ROI mapping results were inspected visually at each slice for accuracy. R2*, FA, and MD values were calculated by averaging mean intensities from right- and left-side ROIs.
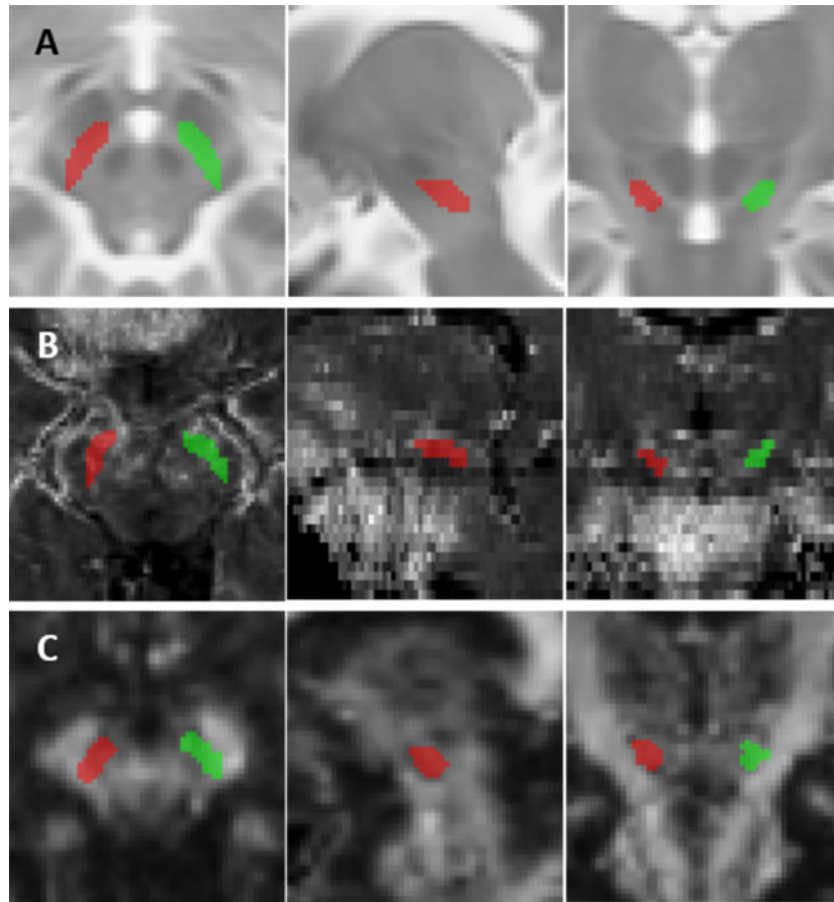
Figure 2. Substantia nigra pars compacta (SNc) segmentation and mapping results. SNc regions of interest (ROI) overlaid on axial, sagittal, and coronal (left to right) images of the midbrain. (A) Right (green) and left (red) SNc ROIs on an MNI152 T2-weighted template. (B) Transverse relaxation rate (R2*) and (C) fractional anisotropy (FA) images from a representative subject with SNc ROI mapping results.

Statistical analyses. Pearson's chi-square test was used to test the difference in H63D allele frequencies between paraquat-exposed and unexposed groups, and the overall difference in the proportions of subjects with "other pesticide/solvent use." The overall group difference in age was tested using a 1-way analysis of variance (ANOVA) with post hoc comparisons. Among the paraquat-exposed subjects, the paraquat-exposure metric was compared between *HFE* wildtypes and H63D carriers using a two-sided *t* test. Overall group and pairwise differences in clinical measurements (MMSE, MoCA, UPSIT, and UPDRS Parts I-III), iron panel measures, and DTI (FA and MD) metrics were tested using 1-way analyses of covariance (ANCOVA) with adjustments for age and "other pesticide/solvent use." R2* measurements were compared using a 1-way ANCOVA with adjustments for age and "other pesticide/solvent use," but also included a study variable covariate to account for possible differences in MRI acquisition between the two originating cohorts. Associations between serum iron panel, R2*, and DTI measurements were tested separately among unexposed and paraquat-exposed groups using Pearson's partial correlation. Associations were examined by correlating residuals after regressing each variable on age; R2* residuals were obtained by regressing on both age and the study variable. All statistical analyses were performed using R version 3.4.2 (R Core Team, Vienna, Austria). Due to the

explorative nature of the study, we did not control for multiple comparisons.

RESULTS

Demographics and Clinical Measurements

Overall, 27 of the 69 study subjects were heterozygous carriers of the H63D variant. Among the unexposed subjects, 21 were *HFE* wildtype, 18 were H63D heterozygous, and 2 were C282Y heterozygous (Table 1). Among the paraquat-exposed subjects, 16 were *HFE* wildtype, 9 were H63D heterozygous, and 3 were C282Y heterozygous. No subjects were H63D or C282Y homozygous, or compound heterozygous. H63D allele frequencies were not different between unexposed and exposed subjects (*p* value = .422). There was no group difference in age between exposed and unexposed subjects, although unexposed wildtypes trended younger on average than both unexposed H63D carriers (*p* value = .066) and paraquat-exposed wildtypes (*p* value = .082). Adjustments for age were made, therefore, in all subsequent group comparisons.

Paraquat exposure duration did not differ between exposed wildtypes and H63D carriers (*p* value = .747). Proportions of "other pesticide/solvent use" among subjects differed between groups (*p* value < .001). Usage of other chemicals was associated

Table 1. Demographic and Clinical Measures for Study Participants

	HFE$^{+/+}$		HFE$^{+/H63D}$		
	Unexposed	Exposed	Unexposed	Exposed	p
N (with MRI)[a]	21 (20)	16 (15)	18 (17)	9 (8)	.422
Age (years)[b]	50.5 ± 3.1	57.4 ± 2.2	57.8 ± 2.1	48.0 ± 5.3	.845
Paraquat exposure metric[c]	—	11.6 ± 1.8	—	10.6 ± 2.5	.747
Other pesticide/solvent use[a]	10 (47.6%)	16 (100%)	8 (44.4%)	9 (100%)	<.001
MMSE[d]	28.7 ± 0.4	28.3 ± 0.3	28.9 ± 0.2	28.1 ± 0.5	.235
MoCA[d]	26.0 ± 0.7	25.6 ± 0.9	25.5 ± 0.5	26.6 ± 0.8	.742
UPSIT[d]	33.6 ± 0.9	32.0 ± 1.3	33.4 ± 1.4	34.0 ± 1.1	.767
UPDRS scores[d]					
Part I	5.0 ± 0.8	4.9 ± 1.0	3.9 ± 1.0	3.2 ± 0.7	.402
Part II	0.6 ± 0.2	0.6 ± 0.2	0.2 ± 0.2	0.6 ± 0.2	.904
Part III	1.3 ± 0.4	4.6 ± 0.7	3.2 ± 0.7	2.8 ± 1.2	.012

Statistical tests used: [a]Chi-square test; [b]ANOVA; [c]2-sided t test; [d]ANCOVA with adjustments for age.

Abbreviations: *HFE*, homeostatic iron regulator; H63D, histidine to aspartic acid substitution at position 63; MMSE, Mini-Mental Status Exam; MoCA, Montreal Cognitive Assessment; UPSIT, University of Pennsylvania Smell Identification Test; UPDRS, Unified Parkinson's Disease Rating Scale.
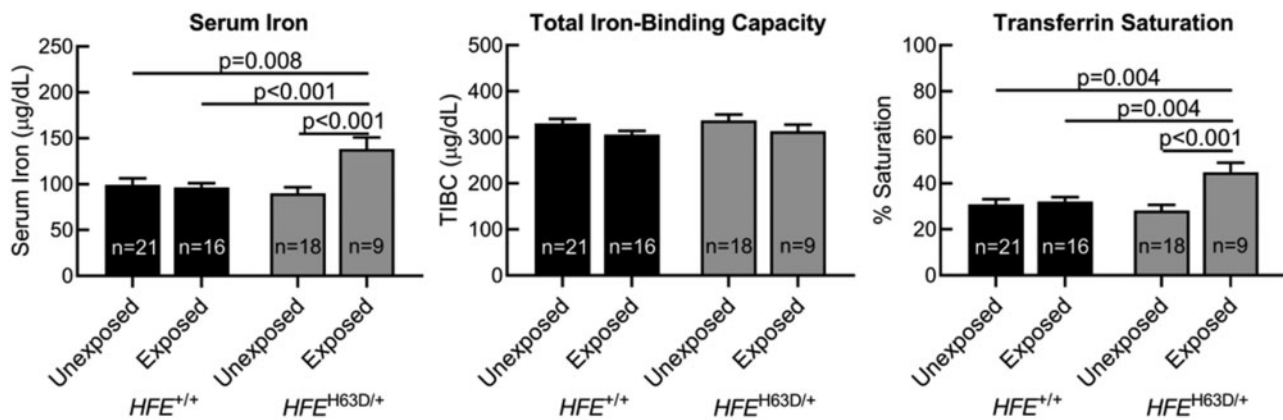
Figure 3. Group differences in serum iron panel measurements. Comparisons of serum iron panel measurements by *HFE* genotype and paraquat exposure. Subjects were grouped by *HFE* genotype (*HFE*$^{+/+}$ vs *HFE*$^{H63D/+}$) and history of paraquat exposure (unexposed vs exposed). *p* values reflect adjustments for "other pesticide/solvent use" and age.

with paraquat exposure, but not *HFE* genotype (Supplementary Table 1). No subjects had previous history of other PD-associated pesticide, solvent, or lead poisoning. MMSE, MoCA, UPSIT, and UPDRS Parts I-II were similar across groups and within normal ranges. Unexposed wildtype subjects had lower UPDRS-III scores than both unexposed H63D carriers and paraquat-exposed wildtypes (*p* values < .017), but the difference was not clinically meaningful because all scores were within normal range (Table 1). UPDRS-III did not associate with iron or MRI measurements among paraquat-exposed or unexposed subjects in subsequent correlation analyses (see Associations between Iron and MRI Measurements).
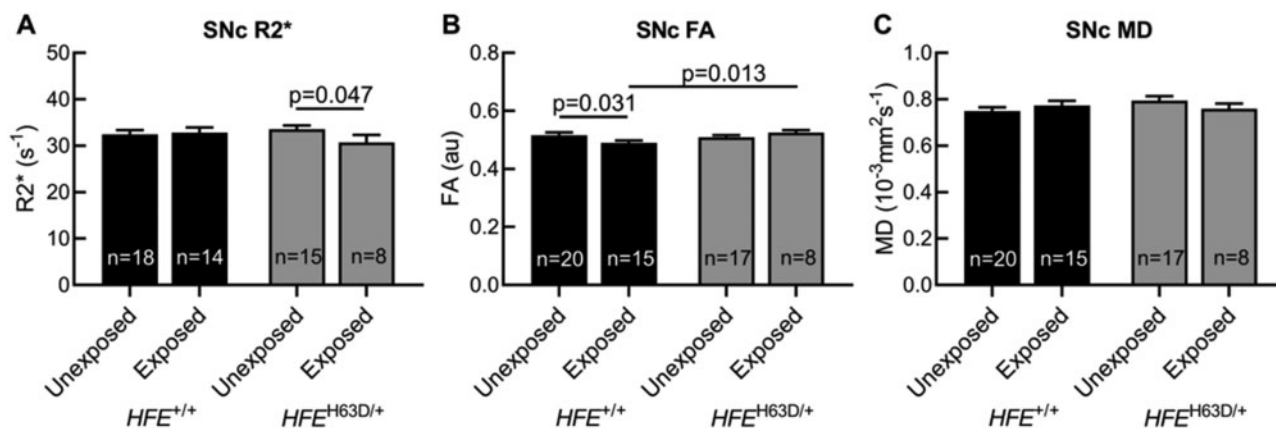
Group Differences in Iron Panel Measurements
Group means for all iron panel measurements were within normal reference ranges (Jackson *et al.*, 2001) (Figure 3). Unexposed *HFE* wildtypes, paraquat-exposed *HFE* wildtypes, and unexposed H63D carriers had similar serum iron levels. Exposed H63D carriers, however, demonstrated significantly higher serum iron than all other groups (*p* values ≤ .008). There were no differences in TIBC between groups. As with serum iron, transferrin saturation was similar in unexposed *HFE* wildtypes,

paraquat-exposed *HFE* wildtypes, and unexposed H63D carriers, but significantly higher in exposed H63D carriers compared with all other groups (*p* values ≤ .004).

Group Differences in SNc MRI Measurements
SNc R2* values were similar in unexposed *HFE* wildtypes, exposed HFE wildtypes, and unexposed H63D carriers. SNc R2* values were lower in paraquat-exposed H63D carriers than in unexposed carriers (*p* value = .047, Figure 4A). SNc FA values were similar in unexposed *HFE* wildtypes, unexposed H63D carriers, and exposed H63D carriers. SNc FA values for exposed *HFE* wildtypes were significantly lower than both unexposed *HFE* wildtypes (*p* value = .031) and exposed H63D carriers (*p* value = .013, Figure 4B). There were no group differences in SNc MD (Figure 4C).

Associations Between Iron and MRI Measurements. After regressing each variable set on age, serum iron, TIBC, and transferrin saturation were not associated with SNc R2*. Serum iron associated positively with SNc FA among paraquat-exposed subjects (*r* = 0.49; *p* value = .014), but not among unexposed subjects (*r* = −0.17; *p* value = .441) (Figure 5). In subgroup analyses, serum

Figure 4. Group differences in MRI measurements. Group differences in substantia nigra pars compacta (SNc) transverse relaxation rate (R2*) and diffusion tensor imaging scalars of fractional anisotropy (FA) and mean diffusivity (MD). Subjects were grouped by *HFE* genotype (*HFE*^{+/+} vs *HFE*[H63D/+]) and history of paraquat exposure (unexposed vs exposed). R2* measurements were compared using 1-way analyses of covariance (ANCOVA) adjusting for "other pesticide/solvent use," age, and originating study. FA and MD metrics were compared using ANCOVAs adjusting for "other pesticide/solvent use" and age.
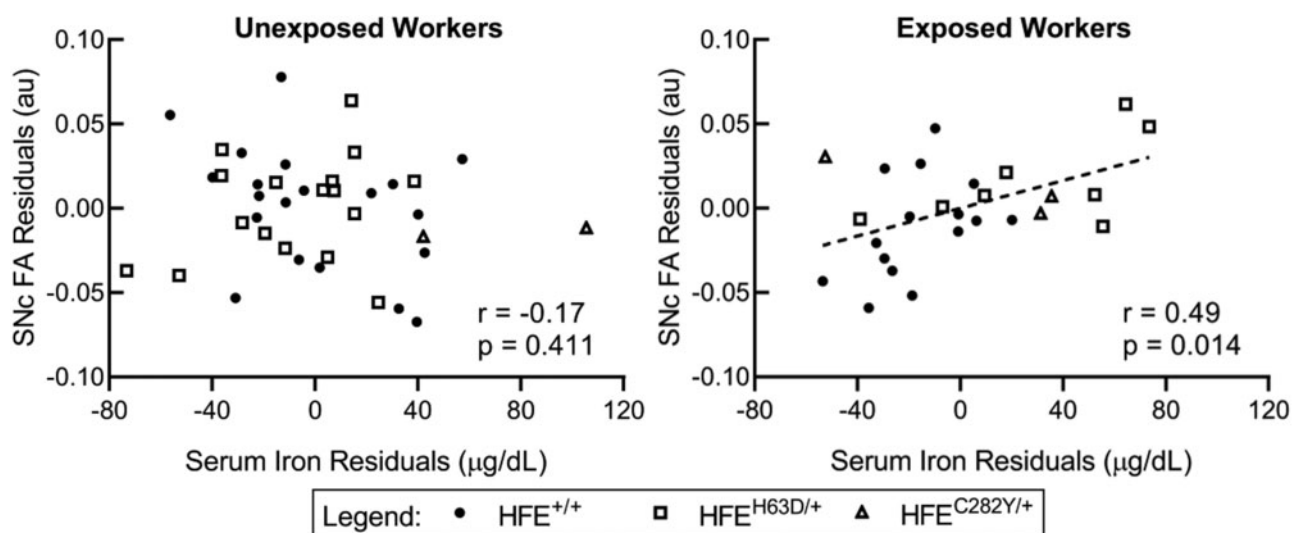
Figure 5. Substantia nigra pars compacta (SNc) fractional anisotropy (FA) residuals versus serum iron residuals. Scatterplots of SNc FA age-regressed residuals against serum iron age-regressed residuals among paraquat-exposed and unexposed workers.

iron and SNc FA also associated positively among paraquat-exposed *HFE* wildtypes ($r = 0.54$; p value = .044), but did not reach statistical significance in exposed H63D carriers ($r = 0.61$; p value = .147). TIBC and transferrin saturation did not associate with SNc FA in exposed or unexposed subjects, although the association between transferrin saturation and SNc FA was trending ($r = 0.38$; p value = .063). SNc MD did not associate with any iron panel measurements. There were no associations between SNc R2* and either SNc FA or MD metrics (Table 2).

DISCUSSION

We observed lower SNc microstructural integrity in paraquat-exposed *HFE* wildtypes, but not in exposed H63D heterozygous carriers. This finding is consistent with our recent observation of H63D-related neuroprotection in mice (Nixon *et al.*, 2018), and

provides initial clinical support for a possible gene-environment interaction in paraquat neurotoxicity. Future studies with larger cohorts are warranted to replicate these findings and examine potential underlying mechanisms.

Iron Differences Are Associated With Paraquat Exposure in H63D Carriers

To the best of our knowledge, an interaction of paraquat exposure and H63D status on iron metabolism has not been examined previously. The present study found that serum iron and transferrin saturation were significantly higher in paraquat-exposed H63D subjects than in all other groups. Human studies have shown that H63D heterozygotes have mildly elevated serum iron levels compared with *HFE* wildtypes (Jackson *et al.*, 2001), and H63D homozygosity is associated with elevated levels of ferritin, the major intracellular iron storage protein (Kelley

Table 2. Associations Between Iron and MRI Measurements

	Unexposed Workers								Exposed Workers							
	Iron		TIBC		Transferrin		R2*		Iron		TIBC		Transferrin		R2*	
	r	p value	r	p value	r	p value	r	p value	r	p value	r	p value	r	p value	r	p value
R2*	−0.04	0.826	0.04	0.844	−0.04	0.829	—	—	−0.20	0.352	0.17	0.420	−0.26	0.213	—	—
FA	−0.14	0.412	−0.05	0.783	−0.15	0.376	−0.08	0.710	**0.49**	**0.014**	0.16	0.440	0.38	0.063	0.00	0.981
MD	−0.15	0.378	0.18	0.285	−0.14	0.388	−0.13	0.454	−0.11	0.604	0.09	0.684	−0.11	0.611	−0.16	0.352

Pearson correlation coefficients between age-regressed residuals for serum iron panel measurements, substantia nigra pars compacta (SNc) transverse relaxation rate (R2*), and SNc diffusion tensor imaging (DTI) scalars of fractional anisotropy (FA) and mean diffusivity (MD), among paraquat-exposed and unexposed workers. Abbreviation: TIBC, total iron-binding capacity.

et al., 2014). *In vitro*, reduction of paraquat by NADPH has been shown to promote the reductive release of iron from purified ferritin (Thomas and Aust, 1986). Given larger iron stores in H63D carriers, one possible explanation is that paraquat may mobilize iron into peripheral circulation to raise both serum iron and transferrin saturation.

Interestingly, SNc R2* was lower in paraquat-exposed H63D carriers than in unexposed carriers. In our previous study of the murine homolog to H63D (*Hfe* H67D) (Nixon et al., 2018), Perls' staining revealed no difference in SN iron levels between paraquat- and saline-treated *Hfe* H67D mice. Within the SNc, however, paraquat-treated *Hfe* H67D mice had lower staining for L-ferritin, the predominant form of iron storage in glial cells (Han et al., 2002), than their saline-treated H67D counterparts (Nixon et al., 2018). This latter finding supports a paraquat-driven effect on SNc iron homeostasis among H63D carriers, although the mechanisms by which these changes occur are unclear.

Current concepts of brain iron metabolism argue against a direct cause-effect relationship between peripheral and brain iron levels because peripheral iron does not freely traffic across the blood-brain barrier (BBB). Brain iron homeostasis is regulated tightly by the BBB and is relatively independent from iron levels in the periphery (Belaidi and Bush, 2016; Simpson et al., 2015). Consistent with this understanding, we observed no associations (Table 2) and differential responses between SNc R2* and any serum iron panel measurement.

DTI as a Marker for SNc Microstructural Change

Epidemiological and animal studies have provided growing evidence that paraquat inflicts SNc neurotoxicity and is a risk factor for PD development (Bastias-Candia et al., 2019; Tangamornsuksan et al., 2019). In humans, regional case-control studies have shown that paraquat exposure is associated with larger odds for having PD (Hertzman et al., 1990; Pezzoli and Cereda, 2013; Tanner et al., 2011; Wang et al., 2011), and that odds may even increase with greater years of exposure (Liou et al., 1997). In animals, paraquat exposure has been shown to induce reproducible losses in SNc neurons, degeneration of dopaminergic axon terminals, and synaptic alterations (Bove et al., 2019; Brooks et al., 1999; Manning-Bog et al., 2002; Ossowska et al., 2005). Our previous DTI study of asymptomatic agricultural workers revealed that paraquat use is associated with worse SNc FA in a pattern reminiscent of PD (Du et al., 2014). The present study recapitulated this result using an expanded cohort, showing that paraquat-exposed *HFE* wildtype subjects had lower SNc FA than their unexposed *HFE* wildtype counterparts.

Whether SNc FA directly reflects SNc neuron density is unknown. DTI captures the various water diffusion properties of tissues, and typically is used to map white matter tracts. FA reflects the directional dependence of water diffusion that is restricted in axons. Gray matter structures, such as the SNc, have limited axon bundles and therefore relatively low FA values (Alexander et al., 2007; Vaillancourt et al., 2009). Studies have shown that nigral FA declines with disease duration in clinically diagnosed PD (Zhang et al., 2016). As such, it is believed that lower FA values reflect SNc neuron loss, although most have referred to these gray matter changes as losses in microstructural integrity because the exact cellular changes are yet uncharacterized (Alexander et al., 2007; Vaillancourt et al., 2009).

H63D Carriers Exposed to Paraquat Have Preserved SNc Microstructural Integrity

Paraquat-exposed and unexposed H63D carriers did not display a significant difference in SNc FA. This finding is consistent with our previous results (Nixon et al., 2018) that showed mice expressing *Hfe* H67D demonstrated no difference in SNc dopaminergic neuron staining between control and paraquat-treated groups. *Hfe* wildtype mice, however, lost over half of their SNc neurons with paraquat treatment. This loss correlated with poorer performance in motor function tests compared with saline-treated mice. Interestingly, H67D mice also had significantly lower baseline SNc neuron staining compared with wild-type mice, but this did not result in any motor function loss. In the present study, there was no difference in SNc FA values between unexposed wildtypes and unexposed H63D carriers. It is important to note, however, that the study of Nixon et al. (2018) used homozygous H67D-knockin mice, whereas all H63D carriers in the present study were heterozygous.

Altered Iron Homeostasis and Antioxidant Responses to Paraquat Exposure

Serum iron associated positively with SNc FA among all paraquat-exposed workers (Figure 5). Subgroup analyses showed that the association was not driven solely by distinct genotype differences in each measurement. Serum iron also positively associated with SNc FA in both subgroups, but only reached statistical significance in exposed *HFE* wildtypes. Overall, these data suggest that a peripheral iron-related response may limit vulnerability of the SNc to paraquat, regardless of genotype.

A possible explanation for this finding is that peripheral iron changes may confer resistance to paraquat by enhancing antioxidant responses. This hypothesis is supported by early research on paraquat toxicity in plants. As in mammals, paraquat

exerts toxicity in plants through redox cycling. Its site of action is the chloroplast, where it interferes with ferredoxin, an electron carrier component, by competing for electrons with the primary acceptor, $NADP^+$. Once reduced, paraquat interacts with oxygen to yield $O_2^{\bullet-}$. Some plant species (eg, *Hordeum glaucum)* exhibit resistance to paraquat through their ability to translocate the herbicide away from chloroplasts, thereby restricting its redox activity. Others (eg, *Conyza bonariensis*) are naturally resistant due to higher baseline expressions of SOD and other ROS-degrading enzymes (ie, catalase and peroxidases) (Hawkes, 2014). Interestingly, early studies reported the induction of paraquat-resistance in plants after preconditioning them with sublethal doses of iron sulfate and/or other redox agents. These treatments and resultant resistances were associated with enhanced expression of ROS-degrading enzymes (Hoffman, 1978; Lewinsohn and Gressel, 1984; Rabinowitch and Fridovich, 1985).

Our recent data from *Hfe* H67D knock-in mice (Song *et al.,* 2020) suggests that altered iron homeostasis may enhance antioxidative mechanisms in the brain as well. Primary astrocytes cultured from H67D mice were less vulnerable to paraquat than astrocytes from *Hfe* wildtypes (Song *et al.,* 2020). H67D mice previously were found to have increased expression of nuclear factor erythroid 2-related factor 2 (Nrf2), a transcription factor at the center of endogenous antioxidant responses (Nandar *et al.,* 2013). Compared with mouse *Hfe* wildtype astrocytes, H67D astrocytes exhibited a greater increase in nuclear Nrf2 expression following paraquat exposure. They also showed higher levels of the Nrf2 target NAD(P)H quinone dehydrogenase 1 (NQO1), an inducible antioxidant. It is interesting that H63D carriers in the Parkinson's Progression Markers Initiative clinical study also had higher NQO1 levels in their cerebrospinal fluid (Song *et al.,* 2020). Given these previous data, future studies are warranted to investigate whether paraquat resistance may be mediated through iron mobilization, or antioxidant mechanisms in the periphery and/or brain.

Limitations and future directions

The study leveraged existing data to provide an initial test of a novel hypothesis based on recent preclinical findings (Nixon *et al.,* 2018). One major limitation was sample size and genotype representation. The results, however, are consistent with our recent preclinical finding of potential neuroprotective effects from the H63D variant. Future studies with larger cohorts are warranted to test this novel hypothesis more rigorously. Second, the groups trended toward imbalanced mean ages. Age is known to affect both iron levels and FA. Though we adjusted for age in all comparisons and tests for associations, future studies will benefit from matched cohorts. Third, the present cohort only included males though females represent a large fraction of the agricultural workforce. Future studies will prioritize female recruitment to examine possible gender differences. Fourth, whereas paraquat is a well-studied risk factor for PD, exposures to other chemicals, particularly pesticides used in combination with paraquat, may have confounded results. A larger cohort will model more adequately combined exposures. Last, H63D and its murine analogue have been shown to modulate levels of other divalent metals (eg, manganese, lead) in the brain and blood (Claus Henn *et al.,* 2011; Fan *et al.,* 2014; Ye and Kim, 2016). As these also are linked to PD (Aschner *et al.,* 2009; Weisskopf *et al.,* 2010), future studies will benefit from measuring possible changes in their levels and assessing their relation to clinical and MRI measures.

CONCLUSIONS

This study demonstrated that the *HFE* H63D variant may protect against paraquat-associated microstructural changes. The finding is of public health significance due to the high prevalence of H63D in the U.S. population (Steinberg *et al.,* 2001). Furthermore, paraquat use in the United States has increased in volume and geographic area over the past decade, despite bans throughout the European Union and phase outs in China and Brazil (Baker, 2016; Donley, 2019). The findings provide new evidence of genetic-based variability in susceptibility to paraquat neurotoxicity and lend clinical support for a gene-environment interaction in PD etiology. Further research is warranted to confirm these findings and explore mechanisms mediating this possible interaction.

SUPPLEMENTARY DATA

Supplementary data are available at *Toxicological Sciences* online.

ACKNOWLEDGMENTS

FUNDING

DECLARATION OF CONFLICTING INTERESTS

The authors declared no potential conflicts of interest with respect to the research, authorship, and/or publication of this article.

REFERENCES

Alexander, A. L., Lee, J. E., Lazar, M., and Field, A. S. (2007). Diffusion tensor imaging of the brain. *Neurotherapeutics* **4,** 316–329.

Aschner, M., Erikson, K. M., Herrero Hernandez, E., and Tjalkens, R. (2009). Manganese and its role in Parkinson's disease: From transport to neuropathology. *Neuromol. Med*. **11,** 252–266.

Atkinson-Clement, C., Pinto, S., Eusebio, A., and Coulon, O. (2017). Diffusion tensor imaging in Parkinson's disease: Review and meta-analysis. *NeuroImage Clin.* **16**, 98–110.

Baker, N. T. (2016). Agricultural pesticide use estimates for the USGS National Water Quality Network. US Geological Survey Data Release. Available at: https://water.usgs.gov/nawqa/pnsp/usage/maps/show_map.php?year=2016&map=PARAQUAT&hilo=H. Accessed February 8, 2020.

Bastias-Candia, S., Zolezzi, J. M., and Inestrosa, N. C. (2019). Revisiting the paraquat-induced sporadic Parkinson's disease-like model. *Mol. Neurobiol.* **56**, 1044–1055.

Belaidi, A. A., and Bush, A. I. (2016). Iron neurochemistry in Alzheimer's disease and Parkinson's disease: Targets for therapeutics. *J. Neurochem.* **139**, 179–197.

Benyamin, B., McRae, A. F., Zhu, G., Gordon, S., Henders, A. K., Palotie, A., Peltonen, L., Martin, N. G., Montgomery, G. W., Whitfield, J. B., et al. (2009). Variants in TF and HFE explain approximately 40% of genetic variation in serum-transferrin levels. *Am. J. Hum. Genet.* **84**, 60–65.

Betarbet, R., Sherer, T. B., MacKenzie, G., Garcia-Osuna, M., Panov, A. V., and Greenamyre, J. T. (2000). Chronic systemic pesticide exposure reproduces features of Parkinson's disease. *Nat. Neurosci.* **3**, 1301–1306.

Bove, C., Coleman, F. H., and Travagli, R. A. (2019). Characterization of the basic membrane properties of neurons of the rat dorsal motor nucleus of the vagus in paraquat-induced models of parkinsonism. *Neuroscience* **418**, 122–132.

Brooks, A. I., Chadwick, C. A., Gelbard, H. A., Cory-Slechta, D. A., and Federoff, H. J. (1999). Paraquat elicited neurobehavioral syndrome caused by dopaminergic neuron loss. *Brain Res.* **823**, 1–10.

Caballero, M., Amiri, S., Denney, J. T., Monsivais, P., Hystad, P., and Amram, O. (2018). Estimated residential exposure to agricultural chemicals and premature mortality by Parkinson's disease in Washington state. *Int. J. Environ. Res. Public Health* **15**, 2885.

Carocci, A., Catalano, A., Sinicropi, M. S., and Genchi, G. (2018). Oxidative stress and neurodegeneration: The involvement of iron. *Biometals* **31**, 715–735.

Cheng, H. C., Ulane, C. M., and Burke, R. E. (2010). Clinical progression in Parkinson disease and the neurobiology of axons. *Ann. Neurol.* **67**, 715–725.

Cicchetti, F., Lapointe, N., Roberge-Tremblay, A., Saint-Pierre, M., Jimenez, L., Ficke, B. W., and Gross, R. E. (2005). Systemic exposure to paraquat and maneb models early Parkinson's disease in young adult rats. *Neurobiol. Dis.* **20**, 360–371.

Claus Henn, B., Kim, J., Wessling-Resnick, M., Tellez-Rojo, M. M., Jayawardene, I., Ettinger, A. S., Hernandez-Avila, M., Schwartz, J., Christiani, D. C., Hu, H., et al. (2011). Associations of iron metabolism genes with blood manganese levels: A population-based study with validation data from animal models. *Environ. Health Glob.* **10**, 97.

Coban, A., and Filipov, N. M. (2007). Dopaminergic toxicity associated with oral exposure to the herbicide atrazine in juvenile male c57bl/6 mice. *J. Neurochem.* **100**, 1177–1187.

Cocheme, H. M., and Murphy, M. P. (2008). Complex i is the major site of mitochondrial superoxide production by paraquat. *J. Biol. Chem.* **283**, 1786–1798.

Cook, A., Breckenridge, C., Sturgess, N., Minnema, D., Travis, K., and Botham, P. (2014). Letter to the editor. Re: The perplexing paradox of paraquat: The case for host-based susceptibility and postulated neurodegenerative effects. *J. Biochem. Mol. Toxicol.* **28**, 289–290.

Costello, S., Cockburn, M., Bronstein, J., Zhang, X., and Ritz, B. (2009). Parkinson's disease and residential exposure to maneb and paraquat from agricultural applications in the central valley of California. *Am. J. Epidemiol.* **169**, 919–926.

Donley, N. (2019). The USA lags behind other agricultural nations in banning harmful pesticides. *Environ. Health* **18**, 44.

Du, G., Lewis, M. M., Sterling, N. W., Kong, L., Chen, H., Mailman, R. B., and Huang, X. (2014). Microstructural changes in the substantia nigra of asymptomatic agricultural workers. *Neurotoxicol. Teratol.* **41**, 60–64.

Fan, G., Du, G., Li, H., Lin, F., Sun, Z., Yang, W., Feng, C., Zhu, G., Li, Y., Chen, Y., et al. (2014). The effect of the hemochromatosis (HFE) genotype on lead load and iron metabolism among lead smelter workers. *PLoS One* **9**, e101537.

Feder, J. N., Tsuchihashi, Z., Irrinki, A., Lee, V. K., Mapa, F. A., Morikang, E., Prass, C. E., Starnes, S. M., Wolff, R. K., Parkkila, S., et al. (1997). The hemochromatosis founder mutation in HLA-H disrupts beta2-microglobulin interaction and cell surface expression. *J. Biol. Chem.* **272**, 14025–14028.

Filipov, N. M., Stewart, M. A., Carr, R. L., and Sistrunk, S. C. (2007). Dopaminergic toxicity of the herbicide atrazine in rat striatal slices. *Toxicology* **232**, 68–78.

Fitzmaurice, A. G., Rhodes, S. L., Cockburn, M., Ritz, B., and Bronstein, J. M. (2014). Aldehyde dehydrogenase variation enhances effect of pesticides associated with Parkinson disease. *Neurology* **82**, 419–426.

Gash, D. M., Rutland, K., Hudson, N. L., Sullivan, P. G., Bing, G., Cass, W. A., Pandya, J. D., Liu, M., Choi, D. Y., Hunter, R. L., et al. (2008). Trichloroethylene: Parkinsonism and complex 1 mitochondrial neurotoxicity. *Ann. Neurol.* **63**, 184–192.

Gochee, P. A., Powell, L. W., Cullen, D. J., Du Sart, D., Rossi, E., and Olynyk, J. K. (2002). A population-based study of the biochemical and clinical expression of the h63d hemochromatosis mutation. *Gastroenterology* **122**, 646–651.

Goldman, S. M., Quinlan, P. J., Ross, G. W., Marras, C., Meng, C., Bhudhikanok, G. S., Comyns, K., Korell, M., Chade, A. R., Kasten, M., et al. (2012). Solvent exposures and Parkinson disease risk in twins. *Ann. Neurol.* **71**, 776–784.

Gray, J. P., Heck, D. E., Mishin, V., Smith, P. J., Hong, J. Y., Thiruchelvam, M., Cory-Slechta, D. A., Laskin, D. L., and Laskin, J. D. (2007). Paraquat increases cyanide-insensitive respiration in murine lung epithelial cells by activating an NAD(P)H: Paraquat oxidoreductase: Identification of the enzyme as thioredoxin reductase. *J. Biol. Chem.* **282**, 7939–7949.

Han, J., Day, J. R., Connor, J. R., and Beard, J. L. (2002). H and l ferritin subunit mRNA expression differs in brains of control and iron-deficient rats. *J. Nutr.* **132**, 2769–2774.

Hawkes, T. R. (2014). Mechanisms of resistance to paraquat in plants. *Pest Manag. Sci.* **70**, 1316–1323.

Hentze, M. W., Muckenthaler, M. U., Galy, B., and Camaschella, C. (2010). Two to tango: Regulation of mammalian iron metabolism. *Cell* **142**, 24–38.

Hertzman, C., Wiens, M., Bowering, D., Snow, B., and Calne, D. (1990). Parkinson's disease: A case-control study of occupational and environmental risk factors. *Am. J. Ind. Med.* **17**, 349–355.

Hoffman, O. L. 1978. Herbicide antidotes: From concept to practice. In *Chemistry and Action of Herbicide Antidotes* (F. M. Pallos, J. E. Casida, Eds.), pp. 1–13. Academic Press, New York.

Jackson, H. A., Carter, K., Darke, C., Guttridge, M. G., Ravine, D., Hutton, R. D., Napier, J. A., and Worwood, M. (2001). HFE

mutations, iron deficiency and overload in 10,500 blood donors. *Br. J. Haematol.* **114**, 474–484.

Jeng, M. R., Adams-Graves, P., Howard, T. A., Whorton, M. R., Li, C. S., and Ware, R. E. (2003). Identification of hemochromatosis gene polymorphisms in chronically transfused patients with sickle cell disease. *Am. J. Hematol.* **74**, 243–248.

Jones, B. C., Huang, X., Mailman, R. B., Lu, L., and Williams, R. W. (2014a). The perplexing paradox of paraquat: The case for host-based susceptibility and postulated neurodegenerative effects. *J. Biochem. Mol. Toxicol.* **28**, 191–197.

Jones, B. C., Huang, X., Mailman, R. B., Lu, L., and Williams, R. W. (2014b). Response. *J. Biochem. Mol. Toxicol.* **28**, 291–291.

Kelley, M., Joshi, N., Xie, Y., and Borgaonkar, M. (2014). Iron overload is rare in patients homozygous for the h63d mutation. *Can. J. Gastroenterol. Hepatol.* **28**, 198–202.

Lewinsohn, E., and Gressel, J. (1984). Benzyl viologen-mediated counteraction of diquat and paraquat phytotoxicities. *Plant Physiol.* **76**, 125–130.

Lewis, M. M., Sterling, N. W., Du, G., Lee, E. Y., Shyu, G., Goldenberg, M., Allen, T., Stetter, C., Kong, L., Snipes, S. A., *et al.* (2017). Lateralized basal ganglia vulnerability to pesticide exposure in asymptomatic agricultural workers. *Toxicol. Sci.* **159**, 170–178.

Liou, H. H., Tsai, M. C., Chen, C. J., Jeng, J. S., Chang, Y. C., Chen, S. Y., and Chen, R. C. (1997). Environmental risk factors and Parkinson's disease: A case-control study in Taiwan. *Neurology* **48**, 1583–1588.

Manning-Bog, A. B., McCormack, A. L., Li, J., Uversky, V. N., Fink, A. L., and Di Monte, D. A. (2002). The herbicide paraquat causes up-regulation and aggregation of alpha-synuclein in mice: Paraquat and alpha-synuclein. *J. Biol. Chem.* **277**, 1641–1644.

Nandar, W., Neely, E. B., Unger, E., and Connor, J. R. (2013). A mutation in the HFE gene is associated with altered brain iron profiles and increased oxidative stress in mice. *Biochim. Biophys. Acta* **1832**, 729–741.

Nixon, A. M., Meadowcroft, M. D., Neely, E. B., Snyder, A. M., Purnell, C. J., Wright, J., Lamendella, R., Nandar, W., Huang, X., and Connor, J. R. (2018). HFE genotype restricts the response to paraquat in a mouse model of neurotoxicity. *J. Neurochem.* **145**, 299–311.

Ossowska, K., Wardas, J., Śmiałowska, M., Kuter, K., Lenda, T., Wierońska, J. M., Zięba, B., Nowak, P., Dąbrowska, J., Bortel, A., *et al.* (2005). A slowly developing dysfunction of dopaminergic nigrostriatal neurons induced by long-term paraquat administration in rats: An animal model of preclinical stages of Parkinson's disease? *Eur. J. Neurosci.* **22**, 1294–1304.

Peng, J., Peng, L., Stevenson, F. F., Doctrow, S. R., and Andersen, J. K. (2007). Iron and paraquat as synergistic environmental risk factors in sporadic Parkinson's disease accelerate age-related neurodegeneration. *J. Neurosci.* **27**, 6914–6922.

Peng, J., Stevenson, F. F., Oo, M. L., and Andersen, J. K. (2009). Iron-enhanced paraquat-mediated dopaminergic cell death due to increased oxidative stress as a consequence of microglial activation. *Free Radic. Biol. Med.* **46**, 312–320.

Pezzoli, G., and Cereda, E. (2013). Exposure to pesticides or solvents and risk of Parkinson disease. *Neurology* **80**, 2035–2041.

Pu, Y., Chang, L., Qu, Y., Wang, S., Tan, Y., Wang, X., Zhang, J., and Hashimoto, K. (2020). Glyphosate exposure exacerbates the dopaminergic neurotoxicity in the mouse brain after repeated administration of MPTP. *Neurosci. Lett.* **730**, 135032.

Rabinowitch, H. D., and Fridovich, I. (1985). Growth of chlorella sorokiniana in the presence of sulfite elevates cell content of superoxide dismutase and imparts resistance towards paraquat. *Planta* **164**, 524–528.

Rappold, P. M., Cui, M., Chesser, A. S., Tibbett, J., Grima, J. C., Duan, L., Sen, N., Javitch, J. A., and Tieu, K. (2011). Paraquat neurotoxicity is mediated by the dopamine transporter and organic cation transporter-3. *Pro. Natl. Acad. Sci. U.S.A.* **108**, 20766–20771.

Reczek, C. R., Birsoy, K., Kong, H., Martinez-Reyes, I., Wang, T., Gao, P., Sabatini, D. M., and Chandel, N. S. (2017). A CRISPR screen identifies a pathway required for paraquat-induced cell death. *Nat. Chem. Biol.* **13**, 1274–1279.

Rhodes, S. L., Fitzmaurice, A. G., Cockburn, M., Bronstein, J. M., Sinsheimer, J. S., and Ritz, B. (2013). Pesticides that inhibit the ubiquitin-proteasome system: Effect measure modification by genetic variation in skp1 in Parkinsons disease. *Environ. Res.* **126**, 1–8.

Shimada, H., Hirai, K., Simamura, E., and Pan, J. (1998). Mitochondrial nadh-quinone oxidoreductase of the outer membrane is responsible for paraquat cytotoxicity in rat livers. *Arch. Biochem. Biophys.* **351**, 75–81.

Simpson, I. A., Ponnuru, P., Klinger, M. E., Myers, R. L., Devraj, K., Coe, C. L., Lubach, G. R., Carruthers, A., and Connor, J. R. (2015). A novel model for brain iron uptake: Introducing the concept of regulation. *J. Cereb. Blood Flow Metab.* **35**, 48–57.

Snyder, A. M., and Connor, J. R. (2009). Iron, the substantia nigra and related neurological disorders. *Biochim. Biophys. Acta* **1790**, 606–614.

Song, I. Y., Snyder, A. M., Kim, Y., Neely, E. B., Wade, Q. W., and Connor, J. R. (2020). The nrf2-mediated defense mechanism associated with HFE genotype limits vulnerability to oxidative stress-induced toxicity. *Toxicology* **441**, 152525.

Steinberg, K. K., Cogswell, M. E., Chang, J. C., Caudill, S. P., McQuillan, G. M., Bowman, B. A., Grummer-Strawn, L. M., Sampson, E. J., Khoury, M. J., and Gallagher, M. L. (2001). Prevalence of c282y and h63d mutations in the hemochromatosis (HFE) gene in the United States. *JAMA* **285**, 2216–2222.

Suntres, Z. E. (2002). Role of antioxidants in paraquat toxicity. *Toxicology* **180**, 65–77.

Tangamornsuksan, W., Lohitnavy, O., Sruamsiri, R., Chaiyakunapruk, N., Norman Scholfield, C., Reisfeld, B., and Lohitnavy, M. (2019). Paraquat exposure and Parkinson's disease: A systematic review and meta-analysis. *Arch. Environ. Occup. Health* **74**, 225–238.

Tanner, C. M., Kamel, F., Ross, G. W., Hoppin, J. A., Goldman, S. M., Korell, M., Marras, C., Bhudhikanok, G. S., Kasten, M., Chade, A. R., *et al.* (2011). Rotenone, paraquat, and Parkinson's disease. *Environ. Health Perspect.* **119**, 866–872.

Thomas, C. E., and Aust, S. D. (1986). Reductive release of iron from ferritin by cation free radicals of paraquat and other bipyridyls. *J. Biol. Chem.* **261**, 13064–13070.

Vaillancourt, D. E., Spraker, M. B., Prodoehl, J., Abraham, I., Corcos, D. M., Zhou, X. J., Comella, C. L., and Little, D. M. (2009). High-resolution diffusion tensor imaging in the substantia nigra of de novo Parkinson disease. *Neurology* **72**, 1378–1384.

Waheed, A., Parkkila, S., Zhou, X. Y., Tomatsu, S., Tsuchihashi, Z., Feder, J. N., Schatzman, R. C., Britton, R. S., Bacon, B. R., and Sly, W. S. (1997). Hereditary hemochromatosis: Effects of C282Y and H63D mutations on association with beta2-microglobulin, intracellular processing, and cell surface expression of the HFE protein in COS-7 cells. *Proc. Natl. Acad. Sci. U.S.A.* **94**, 12384–12389.

Wang, A., Costello, S., Cockburn, M., Zhang, X., Bronstein, J., and Ritz, B. (2011). Parkinson's disease risk from ambient exposure to pesticides. *Eur. J. Epidemiol.* **26**, 547–555.

Ward, R. J., Zucca, F. A., Duyn, J. H., Crichton, R. R., and Zecca, L. (2014). The role of iron in brain ageing and neurodegenerative disorders. *Lancet Neurol.* **13**, 1045–1060.

Weisskopf, M. G., Weuve, J., Nie, H., Saint-Hilaire, M. H., Sudarsky, L., Simon, D. K., Hersh, B., Schwartz, J., Wright, R. O., and Hu, H. (2010). Association of cumulative lead exposure with Parkinson's disease. *Environ. Health Perspect.* **118**, 1609–1613.

Ye, Q., and Kim, J. (2016). Mutation in HFE gene decreases manganese accumulation and oxidative stress in the brain after olfactory manganese exposure. *Metallomics* **8**, 618–627.

Yin, L., Lu, L., Prasad, K., Richfield, E. K., Unger, E. L., Xu, J., and Jones, B. C. (2011). Genetic-based, differential susceptibility to paraquat neurotoxicity in mice. *Neurotoxicol. Teratol.* **33**, 415–421.

Zhang, Y., Wu, I. W., Tosun, D., Foster, E., Schuff, N., the Parkinson's Progression Markers Initiative (2016). Progression of regional microstructural degeneration in Parkinson's disease: A multicenter diffusion tensor imaging study. *PLoS One* **11**, e0165540.